

## Evidence of folded acoustic phonon modes in the light scattering spectrum of incommensurate quartz

This article has been downloaded from IOPscience. Please scroll down to see the full text article.

1992 J. Phys.: Condens. Matter 4 9931

(<http://iopscience.iop.org/0953-8984/4/49/021>)

View [the table of contents for this issue](#), or go to the [journal homepage](#) for more

Download details:

IP Address: 171.66.16.159

The article was downloaded on 12/05/2010 at 12:37

Please note that [terms and conditions apply](#).

## Evidence of folded acoustic phonon modes in the light scattering spectrum of incommensurate quartz

M Vallade†, K Abe†§, B Berge† and T Shigenari‡

† Laboratoire de Spectrométrie Physique, Université Joseph Fourier, BP 87, 38402 Saint-Martin-d'Hères Cédex, France

‡ Department of Applied Physics and Chemistry, The University of Electrocommunications, 1-5-1 Chofugaoka, Chofu, Tokyo 182, Japan

Received 6 July 1992, in final form 14 September 1992

**Abstract.** Low-frequency light scattering spectra of the incommensurate phase of quartz show the presence of weak additional peaks in the 6–12  $\text{cm}^{-1}$  range. These peaks are shown to correspond to 'folded' acoustic phonons with a wavevector close to the incommensurate modulation wavevector. A transverse acoustic mode and a longitudinal mode can be identified in the ( $ZZ$ ) and ( $X + Y, Z$ ) polarization configurations, respectively. Selection rules for Raman activation of acoustic modes are derived in the special case of the 'triple- $q$ ' incommensurate structure, and the results are compared with experimental observations.

### 1. Introduction

When atomic positions of a crystal are spatially modulated with a wavelength commensurate with the lattice parameters, the new unit-cell dimension is a multiple of that of the primitive value and the Brillouin zone is folded in the reduced-zone scheme. As a consequence of this reduction in translational symmetry, the phonon modes with a wavevector equal to the modulation wavevector in the primitive crystal become zone-centre modes and they can be observed in Raman or infrared spectroscopy.

This effect has been particularly well evidenced in artificially fabricated superlattices (Jusserand and Cardona 1989) and it has proved to be an interesting way to study the phonon dispersion curves in these systems. In the case of incommensurate modulation there is a full breaking of translational symmetry, and the Brillouin zone of the modulated crystal has a vanishing width along the modulation wavevector direction. Strictly speaking, all the phonon modes with a wavevector along that direction can be optically active. The number of modes with a non-negligible oscillator strength, however, is expected to be small (Janssen 1986). In the case of a weak sinusoidal incommensurate modulation, only the phonon modes with a wavevector close to the modulation wavevector have an observable activity (Dvorak and Petzelt 1978). This can be most simply discussed, in the case of Raman scattering, by

§ Permanent address: The University of Electrocommunications, 1-5-1 Chofugaoka, Chofu, Tokyo 182, Japan.

expanding the dynamical permittivity tensor as a function of the incommensurate order parameter  $\langle Q_{q_0, j_0} \rangle$  (Poulet and Pick 1981):

$$\delta\epsilon_{\alpha\beta} = R_{\alpha,\beta}^{(2)} \begin{pmatrix} q_0 j_0 \\ -q_0, j \end{pmatrix} \langle Q_{q_0, j_0} \rangle Q_{-q_0, j} + \dots \quad (1)$$

In this expression,  $Q_{q,j}$  is a phonon normal coordinate with vector  $q$  and branch index  $j$ ;  $j_0$  corresponds to the soft branch and  $q_0$  is the modulation wavevector. Selection rules for the activation of the  $(-q_0, j)$  phonon in the light scattering spectrum of the incommensurate phase are readily derived from equation (1) by studying the transformation properties of the product  $\langle Q_{q_0, j_0} \rangle Q_{q_0, j}$  under the symmetry operation of the point group of the parent (high-temperature) phase. When  $j$  is the soft branch itself ( $j = j_0$ ), the normal coordinates of the excitations are, in fact, linear combinations of  $Q_{q_0, j_0}$  and  $Q_{-q_0, j_0}$  which are called amplitudons and phasons. When  $j$  is different from  $j_0$ , equation (1) describes the activation of 'hard modes' which correspond to Brillouin zone folding.

Experimental observations of these folded hard modes which are quite common in the case of commensurate modulated phases (e.g. in  $\text{SrTiO}_3$  (O'Shea *et al* 1967),  $\text{TaS}_2$  (Duffey *et al* 1976)) are not so frequent for incommensurate systems. Folded acoustic modes have been observed in  $A_2BX_4$ -type crystals by Raman scattering (Lee and Cummins 1989) and by infrared or submillimetre spectroscopy (Torgashev *et al* 1992) in their commensurate phases and, for some of them, also in their incommensurate phase. The light scattering spectrum of ammonium hydrogen oxalate shows evidence of folded acoustic modes in the high-pressure-induced incommensurate phase (Godet *et al* 1989). In the case of quartz we have also suggested that the new peaks which appear in the incommensurate phase may arise from folded acoustic modes (Berge *et al* 1984a, b, Shionoya *et al* 1986). In this paper we present additional measurements which strongly support this assignment.

## 2. Low-frequency Raman spectrum of incommensurate quartz

Quartz crystals exhibit an incommensurate phase over a small range of temperatures ( $T_c < T < T_i$  with  $T_i \simeq 847$  K and  $T_c \simeq T_i - 1.39$  K) between a hexagonal  $\beta$  high-temperature phase and a trigonal  $\alpha$  low-temperature phase. (For a review of incommensurate quartz see Dolino (1986)). One feature of this incommensurate phase is its 'triple- $q$ ' character: three modulation waves with wavevectors at  $120^\circ$  from each other condense simultaneously. Inelastic neutron scattering experiments (Dolino *et al* 1992) have shown that the incommensurate phase arises from the instability of an overdamped soft phonon corresponding to a mixing of an optic mode with a transverse acoustic (TA1) mode polarized in the basal plane. The modulation wavevectors are close to the Brillouin zone centre ( $|q_0| \simeq 0.03a^*$  (where  $a^*$  is the unit-cell parameter of the reciprocal lattice)). Both the modulus and the direction of these wavevectors change when the temperature is varied between  $T_i$  and  $T_c$ . Raman and Brillouin scattering spectra have been extensively studied in incommensurate quartz (Berge *et al* 1984a, b, Shionoya *et al* 1986, Shigenari *et al* 1987, Abe *et al* 1989). In figure 1 we show the Raman spectra measured by Berge *et al* (1984b) using the  $X(ZZ)Y$  configuration. Above  $T_i$ , and just below  $T_i$ , one can see only the longitudinal acoustic (LA) Brillouin peak and a broad temperature-dependent

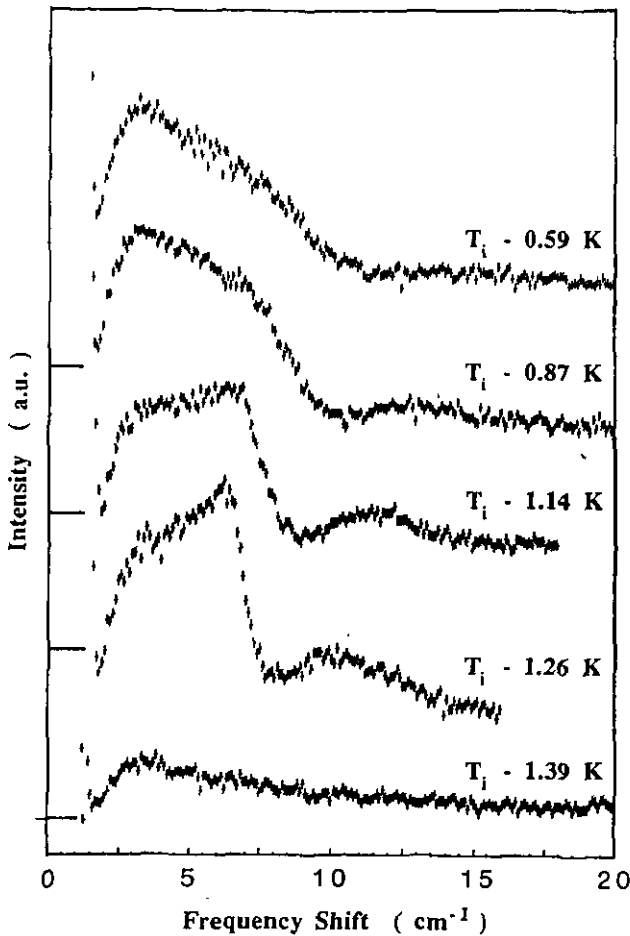


**Figure 1.** Low-frequency ( $ZZ$ ) Raman spectrum of quartz at various temperatures in the incommensurate phase and in the  $\alpha$ -phase (at  $T_i = 1.39$  K, i.e. just below  $T_c$ ) (a.u., arbitrary units). The intensity increase below  $15\text{ cm}^{-1}$  corresponds to the LA Brillouin scattering peak.

central peak. The latter is assigned to a two-phonon Raman scattering process. The sharp dip which is systematically observed on the high-frequency side of the LA peak is interpreted as an interference effect between the LA mode and the broad two-phonon band. (This spectral shape can be quantitatively well interpreted by such a coupled-mode model.) At temperatures below about  $T_i - 0.5$  K, an additional feature appears, the intensity of which increases when approaching  $T_c$ . The shape of this new feature, however, is not simple and a double-peak structure appears close to  $T_c$ . This could indicate the activation of two resonant modes. However, considering the asymmetry of the line profile, it seems more likely that we are again in presence of an interference effect of a single resonant mode with the underlying broad-band peak. Under this latter hypothesis, the resonance frequency of the mode can be approximately determined by subtracting an extrapolated background corresponding to the broad central peak and by taking the intercept of the resulting spectrum with

the frequency axis (figure 2(b)). In the same way, the damping of this mode can be approximately deduced from the separation between the maximum and the minimum obtained in the spectrum after background subtraction. The temperature dependence of the resonance frequency and of the damping determined in this way are shown in figure 2(a).

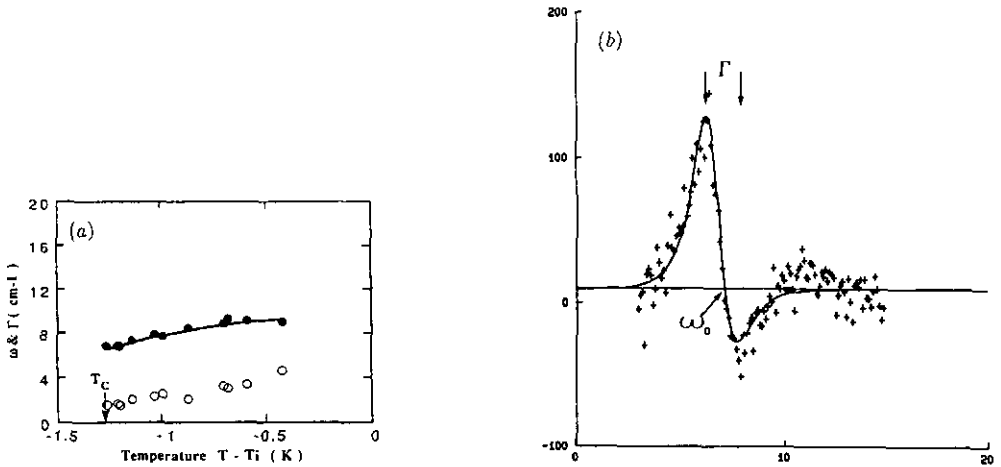


**Figure 2** (a) Temperature dependence of the resonance frequency (●) and of the width (○) of the additional mode observed in the (ZZ) Raman spectrum of incommensurate quartz as deduced using the method in (b); —, calculated frequency of the TA<sub>2</sub> folded acoustic modes. (b) Typical shape of the additional mode observed in the (ZZ) Raman spectrum, after subtraction of an (extrapolated) broad-band central peak. (This shape is interpreted as arising from an interference effect.) The resonance frequency is approximately given by the intercept with the horizontal axis and the width corresponds approximately to the separation between the maximum and the minimum of the spectrum.

In figure 3 are shown new experimental data relative to the  $X(ZX)Y$  geometry. These spectra have been recorded using a 2 m focal length grating monochromator (SOPRA) and an OMA (with light amplifier) detection system. Owing to imperfections in the grating, 'ghosts' of the Brillouin and Rayleigh lines were observed. Their intensities were typically of the order of magnitude of the new peak which appears in the incommensurate phase. Fortunately, as these ghosts appear at temperature-independent frequencies, they can be subtracted. One peak, approximately symmetric, can then be clearly identified. The intensity profile for both Stokes and anti-Stokes peaks was found to be well fitted by a Lorentzian lineshape:

$$I(\omega) = I_0 \left\{ 1/[(\omega - \omega_0)^2 + \Gamma^2] + 1/[(\omega + \omega_0)^2 + \Gamma^2] \right\}. \quad (2)$$

(For an unexplained reason this profile provides a better fit than a damped harmonic oscillator function.) The least-squares fitting procedure leads to a temperature dependence of the parameters  $\omega_0$ ,  $\Gamma$  and  $I_0$  shown in figure 4 and figure 5.

### 3. Analysis of the results and discussion

The analysis of the spectra can be made using the general method described in the introduction. Due care has to be paid, however, to the simultaneous condensation

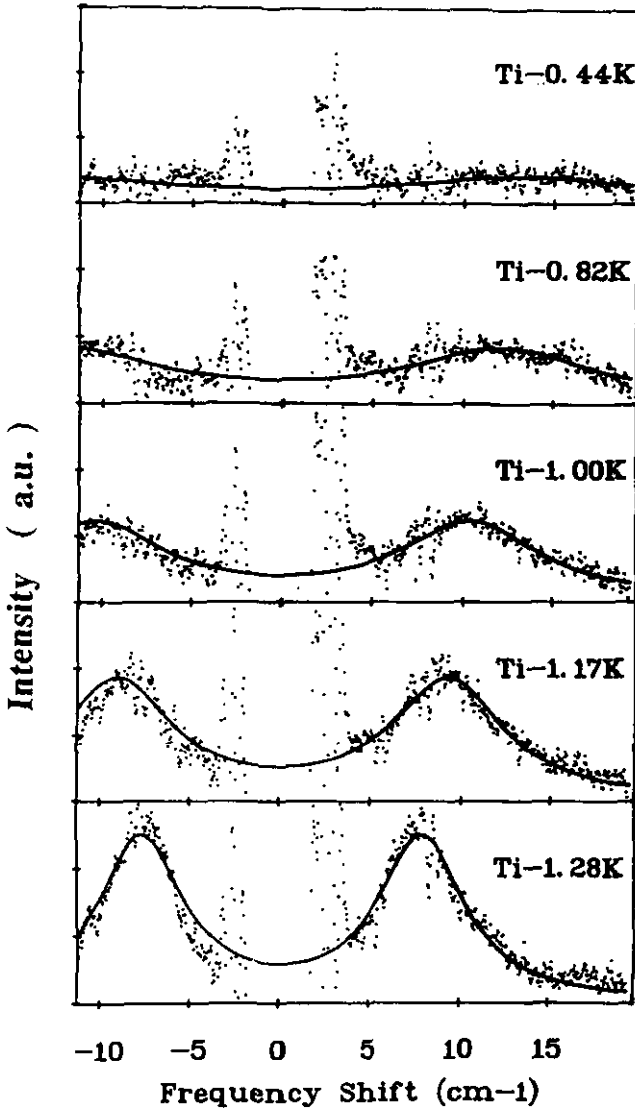


Figure 3. Low-frequency ( $ZX$ ) Raman spectrum of incommensurate quartz at various temperatures (a.u., arbitrary units). A reference spectrum recorded at a temperature just above  $T_i$  has been subtracted from the experimental spectra.

of phonons at six wavevectors  $\pm q_1$ ,  $\pm q_2$  and  $\pm q_3$ , at  $T = T_i$ . As explained in a previous paper (Vallade *et al* 1987), the normal-mode coordinates of the excitations in the incommensurate phase are linear combinations of the six coordinates  $Q_j(q_i)$  corresponding to these six wavevectors. For example, when  $j = j_0$  (the soft-branch index), these excitations can be decomposed into three amplitudons, two gapless phasons and a phason with a gap. Each of these modes transforms as an irreducible representation of the point group  $C_6$  of the incommensurate 'triple- $q$ ' phase and we found that some of them are Raman active. All these soft-mode excitations, however,

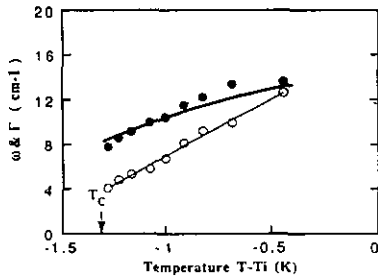


Figure 4. Temperature dependence of the resonance frequency (●) and of the damping constant (○) of the additional mode in the (ZX) Raman spectrum, where the peaks in figure 3 have been fitted using a Lorentzian lineshape: —, calculated frequency of the LA folded acoustic modes.

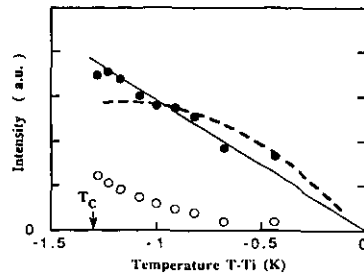


Figure 5. Temperature dependence of the peak intensity (○) and of the integrated intensity (●) of the peaks of figure 3 (fitted using a Lorentzian lineshape) (a.u., arbitrary units): —, best linear fit; ---, temperature dependence of  $\rho^2 q_0^6 / \omega_{LA}^2$ , where  $\rho^2$  is assumed to be proportional to the thermal expansion  $U_{xx}(T)$ .

are expected to be overdamped, since the soft branch itself is found to be overdamped over a large temperature range above  $T_i$  (Dolino *et al* 1992). Therefore they are expected to contribute to the broad central peak. The sharp resonances described in section 2 are more probably due to 'hard modes' on the acoustic branches. Six folded acoustic modes correspond to each branch index  $j$  ( $j = TA1, TA2$  or  $LA$ ). They can be classified according to the irreducible representations of the point group  $C_6$  of the 'triple- $q$ ' incommensurate phase and one finds for each branch the same representation  $A + B_1 + E'_1 + E''_2 + E''_2$  as for decomposition of the soft modes. In principle the frequencies associated with these various components are separated by mini-gaps, but these are expected to be very small as long as the modulation amplitude is not too large. Each folded acoustic mode can then be considered as a set of six quasi-degenerate modes associated with the six representations of the  $C_6$  group. Therefore they are all Raman active, whatever the polarization configuration. Some of them, however, are more active than others. When the modulation amplitude is not too large, the more active modes are those for which the permittivity change  $\Delta\epsilon_{\alpha\beta}$  is linear in the order parameter (see equation (1)). These latter modes can be found by considering the space-group representations of the high-temperature  $\beta$ -phase. TA modes and LA modes at  $q_0$  belong respectively to  $\Sigma_2$  and  $\Sigma_1$  and the soft mode to  $\Sigma_2$ . Since

$$(\Sigma_2)^2 \supset \Gamma_1 + \Gamma_4 + \Gamma_5 + \Gamma_6 \quad \text{and} \quad \Sigma_1 \Sigma_2 \supset \Gamma_2 + \Gamma_3 + \Gamma_5 + \Gamma_6 \quad (3)$$

one concludes that TA folded modes are active in all polarization configurations, and that LA folded modes are only active in configurations (XX), (YY), (XY), (XZ), (YZ). (The activity of LA modes in polarized (ZZ) configurations should appear only in higher-order terms of the order parameter expansion.)

As in quartz the modulation wavevector  $q_0$ , as well as the modulation amplitude  $\rho$ , can be considered as a small quantity, Raman mode activity can also be discussed by considering a  $q_0$  expansion of the permittivity change  $\Delta\epsilon_{\alpha\beta}$ . To lowest order, one can show in particular that the following contributions are symmetry allowed:

$$\begin{aligned}
 (\Delta\epsilon_{zz})_{\text{TA1}} &\propto \rho q_0^2 U_T \\
 (\Delta\epsilon_{zz})_{\text{TA2}} &\propto \rho q_0^3 U_Z \\
 (\Delta\epsilon_{xz}, \Delta\epsilon_{yz})_{\text{TA2}} &\propto \rho q_0^2 U_Z \\
 (\Delta\epsilon_{xz}, \Delta\epsilon_{yz})_{\text{LA}} &\propto \rho q_0^3 U_L.
 \end{aligned}
 \tag{4}$$

( $U_L$ ,  $U_T$  and  $U_Z$  are the atomic displacements in the LA, TA1 and TA2 modes, respectively.) Let us compare these theoretical predictions with our observations.

The peaks observed in the (ZZ) and the (ZX) configurations can be assigned to TA2 and LA folded modes, respectively. This is clearly demonstrated in figure 2 and figure 4, where the observed resonance frequencies are compared with those calculated using the values of the sound velocities  $v$  of the TA2 and LA modes, as measured by Brillouin scattering (Shapiro 1969, Berge *et al* 1984a) and the temperature-dependent incommensurate modulation wavevector  $q_0(T)$  measured by  $\gamma$ -ray diffractometry and neutron scattering (Bastie and Dolino 1985, Mogeon 1988). The agreement between observed and calculated values, which is obtained without any adjustable parameter, strongly supports the present assignment. The small deviations can be explained by the fact that sound velocity dispersion, which is known to exist, has been neglected. For both modes the damping  $\Gamma(T)$  of the folded acoustic modes is found to vary approximately as the square of the resonance frequency  $\omega_0(T)$ . This is the 'normal' behaviour for acoustic phonons ( $\Gamma \sim Dq^2 = (D/v^2)\omega_0^2$ ). The ratio  $\Gamma/\omega_0^2$  is found to be about 0.06 cm for the LA folded acoustic mode and about 0.04 cm for the TA2 folded acoustic mode. These values are in rough agreement with those calculated from Brillouin scattering data at  $T \geq T_i$  (Shapiro 1969, Berge *et al* 1984a). This can be understood by noting that the Landau-Khalatnikov corrections, which are quite important at Brillouin frequencies (about  $1 \text{ cm}^{-1}$ ) in the incommensurate phase, are probably much less important at the folded acoustic mode frequency (about  $6\text{--}10 \text{ cm}^{-1}$ ) so that the ratio  $\Gamma/\omega_0^2$  is expected to be in this latter case approximately the same as that observed above  $T_i$ , where dispersion effects are small.

The temperature dependence of the folded acoustic mode intensity can be reliably deduced only in the case of the depolarized spectrum (see figure 5). Our result is consistent with a linear variation in the integrated peak intensity:  $I_0 \propto T_i - T$ . Small-amplitude and small-modulation wavevector theory predicts that this intensity is proportional to  $\rho^2(T)q_0^6(T)/\omega_0^2(T)$ . Assuming that the temperature dependence of  $\rho^2(T)$  is the same as that of the thermal expansion  $U_{xx}(T)$  (Bachheimer 1980, Mogeon 1988), one actually finds a variation approximately proportional to  $T_i - T$  except close to  $T_c$  where the calculated intensity flattens. This discrepancy could be due to non-negligible contributions from higher-order terms in  $\rho$  and/or to deviations from the simple sinusoidal modulation picture.

According to our above-described analysis, other folded acoustic modes should be observable. The absence of peaks corresponding to the TA1 folded modes can be easily understood because this branch is strongly damped near the modulation wavevector (as a result of its strong coupling to the soft mode (Dolino *et al* 1992)). Therefore TA1 can contribute only to the broad central peak. What is less expected is the lack of a TA2 peak in the depolarized spectrum, since its integrated intensity is predicted to be proportional to  $\rho^2 q_0^4 / \omega_{\text{TA2}}^2$ . No explanation of this fact can at present be given.

To conclude, the low-frequency excitations which have been observed in the



incommensurate phase of quartz can be interpreted as folded acoustic modes. An alternative explanation would be in terms of amplitudons (Shigenari *et al* 1987). In the light of recent inelastic neutron results (Dolino *et al* 1992) it seems very likely that these excitations which arise from the soft-phonon branch are overdamped, and they cannot give rise to the observed underdamped Raman peaks. Furthermore amplitudon frequencies are expected to increase when the temperature is lowered from  $T_i$  to  $T_c$ , whereas the observed modes have a decreasing frequency. When they are interpreted as folded acoustic modes, such a temperature dependence is quite well accounted for as being a consequence of the decrease in the length of the modulation wavevectors.

### Acknowledgment

The authors acknowledge N Sadeghi for his help during the experiments.

### References

- Abe K, Kawasaki K, Koike T and Shigenari T 1989 *J. Phys.: Condens. Matter* **1** 8741  
 Bachheimer J P 1980 *J. Physique Lett.* **41** L559  
 Bastie P and Dolino G 1985 *Phys. Rev. B* **31** 2857  
 Berge B, Dolino G, Vallade M, Boissier M and Vacher R 1984a *J. Physique* **45** 715  
 Berge B, Vallade M and Martinez G 1984b *J. Phys. C: Solid State Phys.* **17** L167  
 Dolino G 1986 *Incommensurate Phases in Dielectrics* vol 2, ed R Blinc and A P Levanyuk (Amsterdam: North-Holland) ch 16  
 Dolino G, Berge B, Vallade M and Moussa F 1992 *J. Physique* **1** 2 1461  
 Duffey J R, Kirby R D and Coleman R V 1976 *Solid State Commun.* **20** 617  
 Dvorak V and Petzelt J 1978 *J. Phys. C: Solid State Phys.* **11** 4827  
 Godet J L, Krauzman M, Pick R M, Poulet H and Toupy N 1989 *J. Physique* **50** 1711  
 Janssen T 1986 *Incommensurate Phases in Dielectrics* vol 1, ed R Blinc and A P Levanyuk (Amsterdam: North-Holland) ch 3  
 Jusserand B and Cardona M 1989 *Topics in Applied Physics* vol 66, ed M Cardona and G Güntherodt (Berlin: Springer) p 48  
 Lee W K and Cummins H Z 1989 *Phys. Rev. B* **39** 4457  
 Mogeon F 1988 *Thesis* Grenoble University  
 O'Shea D C, Kolluri R V and Cummins H Z 1967 *Solid State Commun.* **5** 241  
 Poulet H and Pick R M 1981 *J. Phys. C: Solid State Phys.* **14** 2675  
 Shapiro S M 1969 *Thesis* The Johns Hopkins University, Baltimore  
 Shigenari T, Abe K, Shionoya T, Haga T and Sugiyama M 1987 *Solid State Commun.* **64** 367  
 Shionoya T, Abe K and Shigenari T 1986 *J. Phys. C: Solid State Phys.* **19** 4547  
 Torgashev V I, Latush L T and Yuzuk Yu I 1992 *Ferroelectrics* **125** 129  
 Vallade M, Dvorak V and Lajzerowicz J 1987 *J. Physique* **48** 1171